Combustion Dynamics and Thermal Characterization of a Small LOX/LCH4 Engine for Future Lunar Lander Applications

Austin Morse[1], Pilar Gonzalez Rueda Flores[2], Ahsan Choudhuri[3]

University of Texas at El Paso (UTEP), El Paso, TX, 79968, USA

The Aerospace Center of the University of Texas in El Paso (UTEP) is currently working on a project to design a digital twin of the propulsion system to be used in the development of a prototype small, cargo-focused lunar lander, powered by an array of 500 lbf methane-oxygen engines, dubbed CROME. For this digital twin simulation, computational fluid modeling is used to investigate the combustion dynamics and thermal characteristics of the CROME engine. The engine is simulated within the Siemens Star CCM+ environment to model the steady-state combustion performance, transient start-up sequence and ignition using a torch igniter, and the cooling performance of the fluid film. The combustion of the fuels is modeled using an integrated chemical equilibrium analysis solver with a reduced chemical reaction mechanism file based on Berkeley's GRI-3.0 model. Injection, atomization, and vaporization of the liquid fuels is simulated through a Eulerian multiphase model, with a hybrid Lagrangian model integrated to study droplet formation and vaporization in the transient start-up phase. Finally, a dedicated fluid film model coupled with the multiphase simulates the build-up, flow, and evaporation of the thin fuel film coolant layer along the engine walls. Using these simulation tools, the behavior of a similar rocket engine may be accurately simulated, reducing the time and materials needed for physical testing and accelerating the design and development process.

I. Introduction

One of the biggest developments within the field of propulsion of the last decade has been the proliferation of liquid methane and liquid oxygen as a fuel for rocket engines, due to the fuel combination's high efficiency compared to the more traditional kerosene, its greater density and less severe handling difficulties compared to hydrogen, and the possibility of the combination's synthesis on extraterrestrial environments such as Mars. This combination of parameters makes the combination suitable for applications such as lunar cargo landers, where the combination of storage density and efficiency will enable a lander to carry larger and heavier payloads. However, as with other cryogenic propellant combinations, there are significant modeling and handling difficulties, such as the need for robust multiphase analysis capabilities for cryogenic engine models and the sophisticated insulation and cooling infrastructure required for their storage, especially when considering the long-term storage necessary for interplanetary travel. To ameliorate these difficulties, the modeling of cryogenic propellants, with a focus on liquid oxygen and liquid methane, must be better understood. The final goal of this project is to create a functional digital twin of a conceptual liquid methane-fueled small-scale lunar cargo lander. One of the most important first steps towards this end is the design of an accurate digital model of the lander's engines, capable of assisting validation of engine performance estimates to accelerate the testing process and describing the multiphase behavior of the cryogenic propellants. Through this process, digital testing of the lander system may be accomplished within the Siemens simulation

---

[1] Undergraduate Research Intern, UTEP Aerospace Center, amorse@utep.edu, Student Member, 1314313
[2] Graduate Research Intern, UTEP Aerospace Center, pgonzalez12@miners.utep.edu, Student Member, 1158645
[3] Associate Vice President, UTEP Aerospace Center, ahsan@utep.edu, Associate Fellow, 177825

environment to demonstrate the practicality and use of digital twin modeling and testing for future cryogenically fueled vehicles.

Four major goals exist for this engine simulation: to thermally model the combustion reactions that occur within the engine combustion chamber and resulting gas flow to verify performance estimates, to model the injection, impingement, mixing, and vaporization of the incoming cryogenic liquid fuels, to verify the efficiency of the engine's boundary layer cooling system, and to model the transient start-up sequence of the engine. Due to time constraints, recent progress has been concentrated within the first two goals, with studies into the potential of reduced-order chemical mechanisms for faster combustion simulation and the usage of Eulerian multiphase models to better simulate stratified injection of the liquid fuels. With these improvements, a unified engine model with high-fidelity multiphase and reaction modeling is expected to be possible within the bounds of available computational power.

II. Centennial Restartable Oxygen-Methane Engine (CROME)

The engine currently designed to be used on the lander, named the Centennial Restartable Oxygen-Methane Engine, or CROME, is a small methane-oxygen thruster with limited throttling capability, which utilizes fuel film cooling (FFC) to control thermals at the engine chamber walls, as described in a paper by Herrera [1]. The engine's design is shown in Fig (1). The CROME chamber and nozzle assembly is made of Inconel 718 alloy, while the injector is made of Inconel 625 to take advantage of Inconel's excellent oxidation and corrosion resistance at high temperatures. The engine is rated for a maximum thrust of 500 lbf and a max chamber pressure of 235 psia. Core methane injection is handled through annulus co-axial injection at the center of the injector plate, surrounding a stationary pintle injector through which the liquid oxygen is injected; this method of injection reduces the risk of combustion instability and enhances propellant mixing rate. Methane coolant injection is handled by 17 injection orifices positioned around the injector face's perimeter, angled to impinge upon the chamber wall, which combined deliver 30% of the total methane flow to form the coolant film. Fuel and oxidizer are injected into the chamber at a mixture ratio of 2.7, below the stoichiometric value of 4 to lower combustion temperatures and create a fuel-to-oxidizer volume ratio of 1, allowing for identical tanks to contain both the methane fuel and liquid oxygen. This mixture ratio results in an adiabatic flame temperature of 3209 K, according to the CEA software Cantera using the GRI-Mech 3.0 reaction mechanism [2], with chamber pressure verified using a variation of the choked flow mass flow rate equation, as obtained from Chapter 3 of Sutton [3]. For the atmospheric test model, the engine features a relatively small expansion ratio of 1.7 according to engine specifications described by Herrera [1]. Throttling is accomplished through partial closure of upstream propellant valves, lowering the propellant upstream pressure and decreasing mass flow rate. Throttling is rated at increments of 25% total thrust. The combustion chamber is also flanked by 17 acoustic chambers just below the injector, reducing the risk of combustion instability by damping the expected frequencies of the combustion reaction.

Table 1: CROME Performance and Chamber Parameters

Maximum Thrust	500 lbf
Maximum Chamber Pressure	235 psia
Adiabatic Flame Temperature	3209 K
Expansion Ratio	1.7
Ox. Mass Flow Rate	1.59 lbm/s
Fuel Mass Flow Rate	0.59 lbm/s
FFC Mass Flow rate	0.177 lbm/s
Exit Mach	1.92
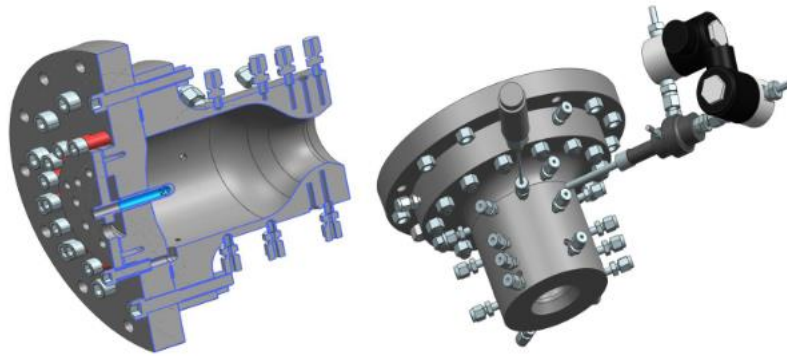
Figure 1: Isometric and Cross-Section Rendering of CROME Engine, with Attached Igniter Torch

III. Engine Model

In order to model flow behavior within the engine, the interior of the engine was modeled within Siemens NX, as shown in Fig. (2). For the initial combustion simulation, only the volume beneath the injector is modeled to reduce model size and complexity, comprising the core chamber volume and short inlets for the methane and oxygen. To reduce complexity further, the model is cut along its plane of symmetry under the assumption of a symmetric process. For some steady-state simulations, this symmetry cut is expanded to a radial cut with a periodic boundary conditions assumption. Both injection areas use velocity flow rate boundary conditions to closely follow the performance parameters detailed by Herrerra [1] without the loss of stability that has been seen with mass flow rate boundaries. The volume is meshed using Star-CCM+'s automated meshing tool, using a polyhedral mesh with a prism layer boundary mesher. The polyhedral mesh allows for better resolution of fluid gradients due to the greater number of cell contact surfaces, while the prism layers are necessary to be able to accurately resolve turbulence effects near the wall. To better accomplish turbulence resolution, the number of prism layers generated is increased to >6, and the prism layer stretching parameter is limited to 1.05-1.2 to create a smoother volume gradient between the prism cells [4].

Figure 2: Engine Model with Fine Polyhedral Mesh

IV. Gas Continuum Modeling

For modeling of the gas continuum, models were chosen to be able to model the compressible flow with an acceptable degree of accuracy and computational speed. For the gaseous equation of state, the ideal gas model is used as it is considered accurate within the operating ranges of the engine and is computationally simple compared to the more robust Real Gas model. To solve the Navier-Stokes equations of the chamber flow, the Reynolds-Averaged Navier-Stokes (RANS) method was used alongside the K-Omega turbulence model for its accuracy in predicting near-wall turbulence, an important factor for boundary layer effects near the chamber walls, affecting both the near-wall flow field and the behavior of the fuel film cooling layer [4]. To accommodate the needs of the multiphase flow model, a segregated solver is used, in which the equations of conservation for mass and momentum are solved sequentially instead of as a combined system. This is generally faster, but less robust than the Coupled Flow solver, especially for supersonic flow [4]. However, as it is required for the later detailed multiphase model, it will be used alongside careful tuning of the equations' under-relaxation parameters to work towards stable convergence.

V. Combustion Modeling

One of the many capabilities offered by Star-CCM+ is the modeling of the finite-rate chemistry between components of a fluid mixture through the cell-wise evaluation of chemical reaction rates [4]. Star-CCM+ offers two different overarching models for chemistry calculations: Reacting Species Transport Models (RSTM), in which the conservation equations for each chemical species are calculated individually, and Flamelet models, in which the conservation equations are calculated for a reduced number of general chemical reaction factors, primarily the mixture fraction and mixture fraction variance. Thus, the Flamelet models are generally less computationally intensive than the Reacting Species Transport models. However, the Flamelet models are also less accurate, especially for simulations where the mixing timescale is significant in relations to the reaction timescale, as is generally the case within rocket engine combustion, where the residence time of the reacting fluids is small. Thus, for the purposes of the engine simulation, Reacting Species Transport is considered the superior model category.

Within Reacting Species Transport are two primary reaction models: Complex Chemistry and Eddy Break-Up. The Complex Chemistry model is considered the most computationally accurate and complex model within Star-CCM+, as it uses a stiff ODE solver to solve for the chemical source terms [4]. Through this robust solver, this model can calculate the chemical source terms for equations comprising hundreds of reactions over varying time scales for dozens or more species, making it the best candidate for simulating complex chemical models. The other option, Eddy Break-Up, is more optimized for simpler mechanisms. Eddy Break-Up computes reaction rates based on the assumption that they are dominated by the turbulent mixing rate, kinetic rate or a combination of both. From this, the model uses a more direct equation for the species source terms, without going through the steps of stiff ODE solving as with Complex Chemistry. However, this limits the model to simpler reaction mechanisms, which do not feature stiff reaction equations, generally limiting it to mechanisms with one or two step reactions.

To model the combustion of the gasified fuels in an efficient manner, a few different avenues of simulation were investigated; Complex Chemistry using the Berkely GRI-3.0 Model, Complex Chemistry with the reduced Lu methane-air mechanism, Complex Chemistry with the skeletal BREF methane-oxygen mechanism, and Eddy Break-Up with the skeletal BREF mechanism. The GRI-3.0 model by Berkely is among the most well-known and extensive mechanisms available for the modeling of methane combustion. Comprising 325 modeled reactions and 53 represented chemical species, it was designed as a comprehensive chemical model for the reaction of air with natural gas [5]. Even though the engine's core combustion reaction is purely oxygen-methane, an air-methane mechanism is seen as likely useful due to the possibility of nitrogen reactions being chemically significant for transient simulations of the engine's startup sequence, where atmospheric nitrogen will make up a significant portion of the chemical species in the chamber volume. However, while its accuracy is high, its computational cost due to the large number of reactions and species to be tracked makes it unappealing for application to the transient simulation of a rocket engine, where the computational time required for other areas necessitates the elimination of unnecessary computed variables. This problem is exacerbated by the fact that GRI-3.0 contains several reactions that are generally considered unimportant to methane combustion, either to support mechanisms for other combustion reactions or to support study into specific areas such as flame radiation. Thus, this model was used as the computational baseline, against which a reduced model may be compared to assess accuracy.

The Lu 30 species model, created by Dr. Tianfeng Lu of the University of Connecticut, is a somewhat reduced model based on the GRI-3.0 mechanism to calculate methane-air reactions [6]. This specific model comprises 30 species and 184 reactions: nearly half the complexity of the GRI-3.0 model, while exhibiting better computational fidelity than other further-reduced models. This was accomplished through the application of directed relation graph,

in which the coupling between each species in the reaction are analyzed on a directed graph, with reactions with weak couplings, as determined by a user-defined error tolerance, are eliminated. Under an error tolerance of 0.13, and with the elimination of species related to NO formation, the removal of 23 species and 141 reactions was accomplished with minimal change in combustion characteristics.

The BREF model, detailed in a paper by Franzelli et. all [7], is a highly simplified mechanism comprising just 6 species and 2 reactions: one for methane oxidation, and one for CO-CO2 shift, making it the ideal candidate for optimization with the Eddy Break-Up model. Despite its simplicity, it can predict flame behavior across a wide degree of operating conditions. However, the model is only validated for use of premixed combustion simulations, while this engine model operates under non-premixed conditions.

Each model and mechanism were tested using an identical 2D converging 'tube' geometry, in which CH4 is injected from the top, meeting the bottom-injected O2 at a 90-degree angle before combusting and producing a flame down the length of the 'tube'. Each model was run at steady-state conditions, with an injected oxygen-methane mass ratio of 2.7 to match injection conditions within the engine chamber and utilization of the Coupled Flow model to allow control of convergence through control of the CFL number. Three tests were run for each model and mechanism; one at atmospheric pressure conditions; another at 125 psi gage pressure; and a final at 250 psi gage pressure, to follow likely pressure conditions within the chamber. For each test, a graph of the temperature and ratio of specific heats is extracted from along the length of the generated steady state flame for comparison, shown below. Additionally, ignition delay may be estimated by the length within the tube before the temperature spikes to flame values. Each test was run for approximately 8000 iterations, with a CFL sequence of 0.1 for the first 1000 iterations; CFL of 1 for the next 1000 iterations; CFL of 10 for 2000 iterations; CFL of 100 for 2000 iterations; and CFL of 1000 for the final 2000 iterations. This sequence produced adequate convergence for each test, as defined by no visual difference in the temperature field for the final iterations and a Continuity residual decrease of at least three orders of magnitude. During testing, only the GRI-3.0 and Lu models converged; the BREF model failed to produce steady-state combustion, likely due to the previously mentioned premixed optimization, and thus was discarded. As BREF was the only model to be tested with Eddy Break-Up, Complex Chemistry was left as the model to be used.

According to Figures (3-8), the Lu mechanism closely matches the GRI-3.0 mechanism for the relevant thermodynamic fields. The only notable point of divergence is in the ignition delay at the atmospheric pressure condition, shown in Fig. (3), where the GRI model predicts the flame developing noticeably later than for LU's. However, at other pressure conditions, the models match each other closely in flame shape, and more closely match the shape of the Lu mechanism atmospheric flame, indicating that this result is possibly more accurate. Additionally, adiabatic flame temperature, as represented by the maximum temperature on the color scale, is near-identical across the models for all test cases.
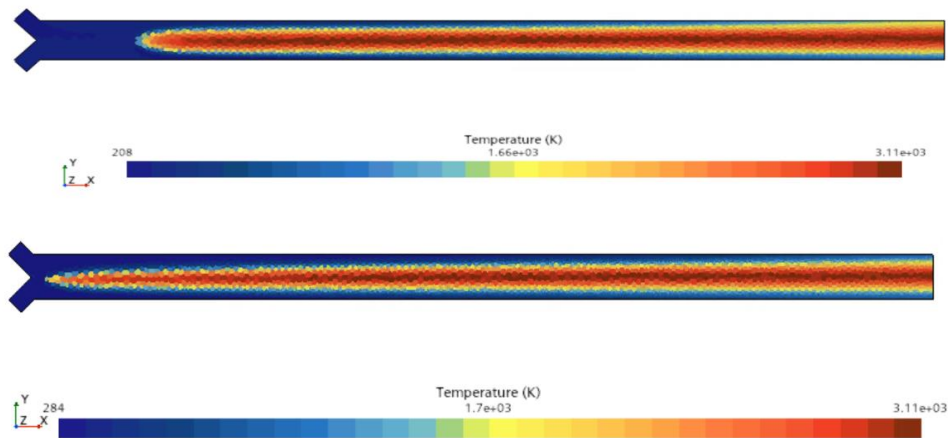
Figure 3: Temperature Fields for GRI-3.0 (Top) and Lu (Bottom) at 0 PSI gage pressure
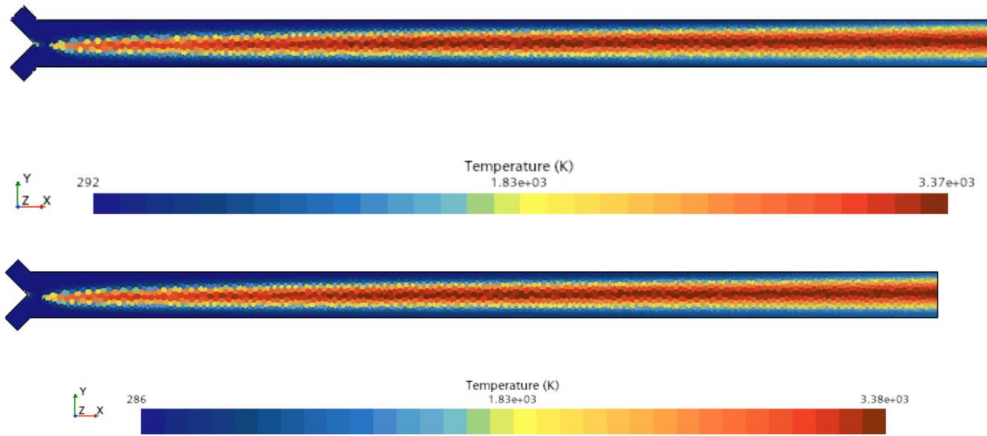
Figure 4: Temperature Fields for GRI-3.0 (Top) and Lu (Bottom) at 125 PSI gage pressure
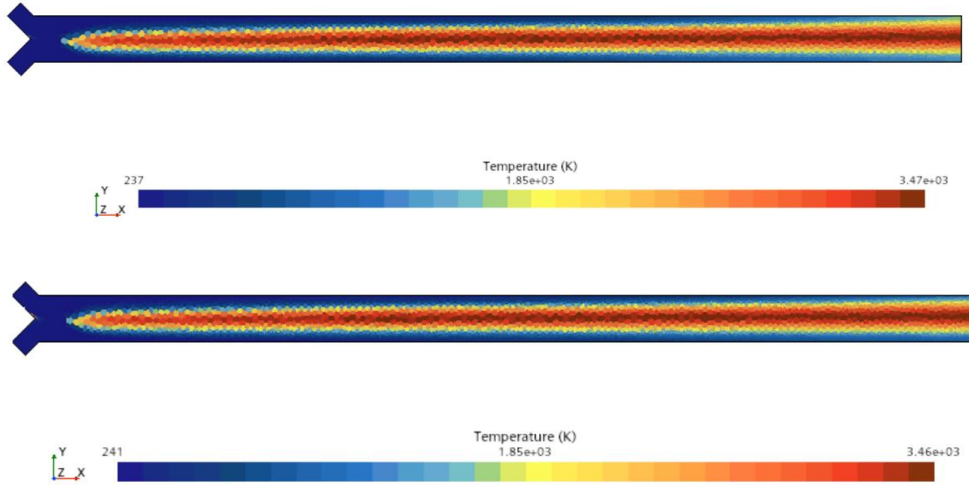
Figure 5: Temperature Fields for GRI-3.0 (Top) and Lu (Bottom) at 250 PSI gage pressure

Additionally, according to the following figures, the composition of the post-combustion gasses is similar enough to produce nearly indistinguishable fields for the ratio of specific heats, indicating extremely similar compressible flow performance between the products of the models.

6
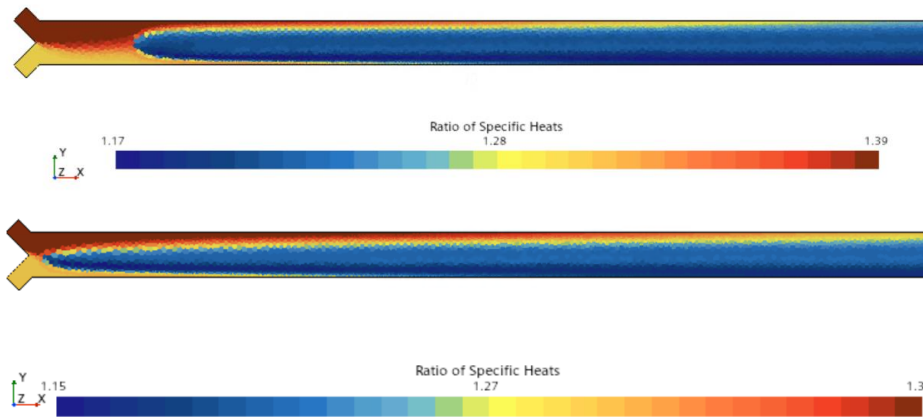
Figure 6: Ratio of Specific Heats Fields for GRI-3.0 (Top) and Lu (Bottom) at 0 PSI gage pressure
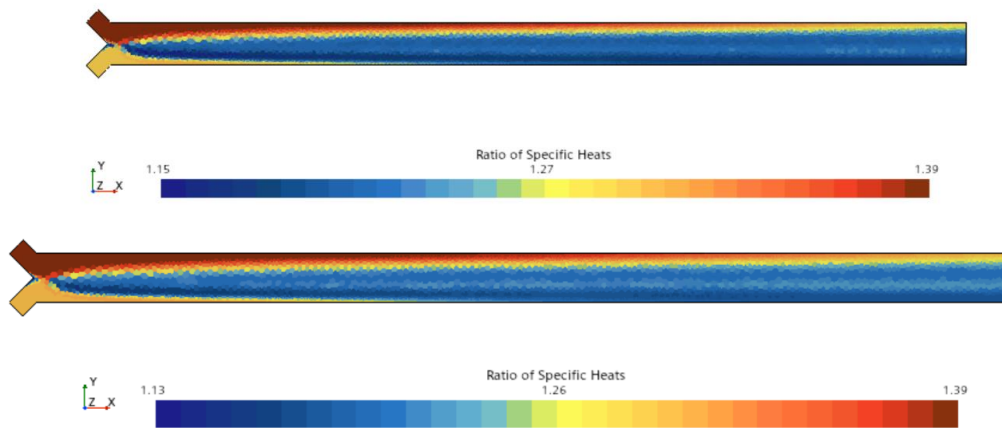
Figure 7: Ratio of Specific Heats Fields for GRI-3.0 (Top) and Lu (Bottom) at 125 PSI gage pressure
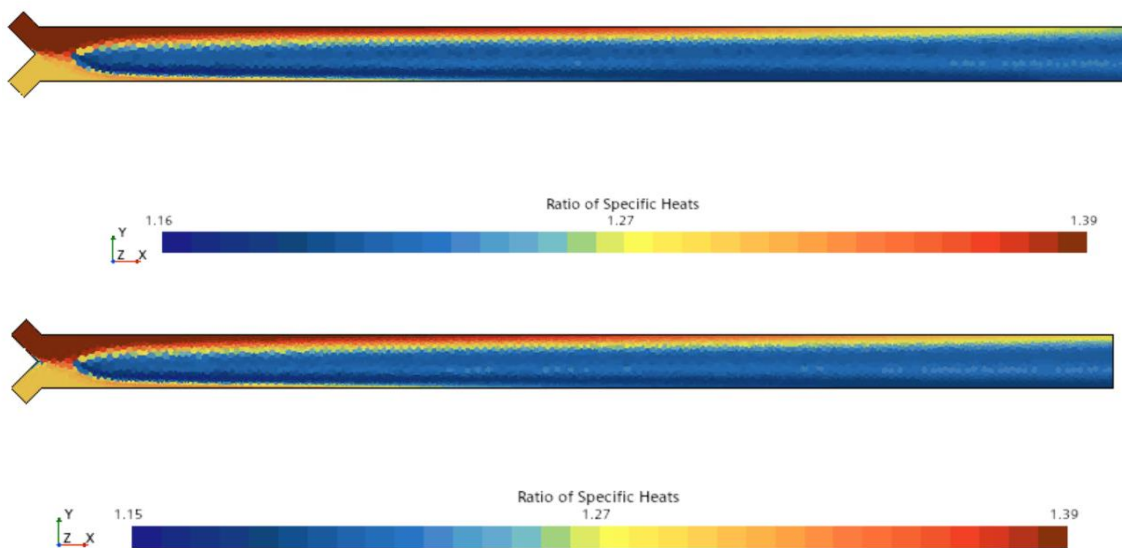
Figure 8: Ratio of Specific Heats Fields for GRI-3.0 (Top) and Lu (Bottom) at 250 PSI gage pressure

From these results, it is sufficiently implied that implementation of the Lu mechanism instead of GRI-3.0 will be capable of accurately modeling the combustion conditions within the engine chamber, allowing for effective simulation of the engine combustion dynamics at a significantly reduced run time. However, despite being greatly reduced compared to GRI, the Lu mechanism is still somewhat computationally heavy compared to other more reduced mechanisms. Thus, further tests with a wider array of mechanisms will be necessary to further optimize combustion simulation.

VI. Multiphase Flow Impingement

To model the injection, impingement, and evaporation of the cryogenic propellants in the gaseous chamber continuum, usage of a multiphase flow model is required. There are two available broad methods to modeling the behavior of multiphase flows: Eulerian methods, in which the phase quality of the fluid is calculated for each cell; and Lagrangian methods, in which one phase is modeled as dispersed particulates traveling through the dominant phase continuum [4]. Previously, the Lagrangian method was used for its relative simplicity. However, this Lagrangian approach was put on hold as the primary method for three reasons: it was highly computationally expensive to track the large number of particles needed to simulate the mass flows of liquid oxygen and methane; it was relatively unstable, with a high dependence on mesh quality and timestep to produce satisfactory flow and impingement behavior without encountering overflow; the particle-based method was reasoned to not be an accurate representative of the liquid injectants, as due to the injector design atomization does not occur until impingement; finally, impingement of the fuel and oxidizer streams was not well-modeled due to the Lagrangian method utilizing a probabilistic algorithm for particle collision which led to much of the propellant streams missing each other entirely. Thus, the modeling of the primary fuel and oxidizer injection was changed to an Eulerian model. The primary models considered for implementation were Eulerian Multiphase, Volume of Fluid, and Mixture Multiphase [4]. For the impingement model, the Volume of Fluid model was chosen, as it was found to model stratified flows with more stability and stratification than the Eulerian Multiphase model and more efficiently than Mixture Multiphase, while the Eulerian Multiphase model was chosen for the final combustion model due to its usage of an enthalpy-based energy equation allowing combustion temperature to be calculated properly.

Improved resolution of the stratified flow is accomplished through the Adaptive Mesh model with the Free Surface Mesh Refinement Criteria. A Maximum Refinement Level of 3 was found to strike the best balance between refinement and computational complexity. Additionally, an Adaptive Timestep was utilized to limit the timestep based on the Courant-Friedrich Levy condition, to ensure stability across timesteps. The Eulerian-Lagrangian resolved transition was processed through a multiphase interaction.

For testing of the multiphase and impingement behavior, a few simplifications were made. First, the full engine model was cut down to an eighth-symmetry slice surrounding the pintle injector to limit the computed area to the immediate vicinity of impingement. Additionally, the gaseous continuum species was cut down to the minimum, representing only O_2, CH_4, and N_2, and reactions were disabled. A fine polyhedral mesh was used to accurately resolve fluid interfaces, with a prism mesh to resolve turbulence. The simulation was run using the unsteady implicit solver, with a timestep of 1E-4 s and 100 iterations per timestep. As required by the VOF multiphase model, segregated solvers were used for the energy, species, phase interactions, and flow equations, with default under-relaxation factors for all. To resolve near-wall turbulence, the k-ω turbulence model was utilized.

For the injection boundaries, a velocity condition was used rather than mass flow rate, as that was found to improve stability for the multiphase injection. Injection velocity was calculated according to the standard equation, in which V is the fluid velocity, ρ is the fluid density, A is the injection area, and $\dot{m}$ is the mass flow rate of the fluid:

$$V = \frac{\dot{m}}{\rho \cdot A} \tag{1}$$

From this, the injection velocity of the methane was found to be 43 m/s, and for the oxygen to be 19.6 m/s. A rotational periodic boundary condition was used to take advantage of the eightfold symmetry to reduce the computational area needed. Atmospheric outlet boundary conditions are used at the interfaces to the rest of the engine, and a standard no-slip wall boundary condition for the injector walls. The phase boundary is represented by an isosurface along which the volume fraction equals 0.5.
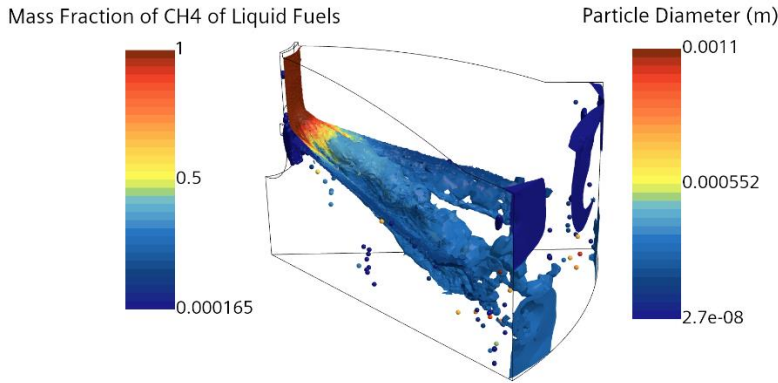
Figure 9: Impingement Pattern of Injected Fuels at t = 2.39 ms

From Figure 9, the impingement pattern at 2.39 ms is shown, demonstrating the behavior of the colliding fluid streams to coalesce into a single wave-like sheet before instabilities cause ligament formation and disintegration beginning closer to the engine walls. Additionally, along the primary sheet the methane volume is shown to be approximately 0.25, close to the predicted optimal value of 0.27 based on the injected OF ration of 2.7, demonstrating decent mixing performance of the pintle-type injector. Further tests may be done with additional cold-flow test data to more accurately assess the efficiency of fuel injection.

VII. Steady-State Combustion

On the path to a full integrated model, an important milestone is the creation and running of a steady-state model integrating multiphase and combustion effects. For this model, the Eulerian Multiphase model was chosen for its better compatibility with calculating combustion temperature through its Segregated Enthalpy energy solver and ability to model dispersed flows without a hybrid model. For this simulation, a further cut-down radial symmetry model in 1/16 symmetry was used to cut down run times on non-HPC systems. Combustion modeling was done with the tested Lu model under the Complex Chemistry solver. As with the impingement tests, the segregated flow solver was used for compatibility. Fluid film deposition is handled through a multiphase interaction between the Film phase in the engine wall shell region and the Eulerian main continuum liquid phase. However, due to compatibility issues, fluid film evaporation is unable to be modeled with the Eulerian Multiphase model; a custom calculation method will have to be developed in order to implement this functionality.

For simulations of the evaporation of the fuel flow in the variable pressure conditions of the engine chamber, saturation pressure is modeled using the Antoine equation, in which P is the saturation pressure, T is the fluid temperature, and A, B, and C are empirical values [4]:

$$P = 10^{(A-\frac{B}{T+C})} \qquad (2)$$

For methane, the values used are A = 3.9895, B = 443.028, and C = -0.49 on a temperature range of 90.99-189.99 K [9], and for oxygen the values used are A = 3.9523, B = 340.024, and C = -4.144 on a temperature range of 54.36-154.33 K [10]. Heat transfer and evaporation of the fluid phase is then handled by the Multicomponent Droplet Evaporation Mass Transfer model, in which droplet evaporation is handled based on the Sherwood Number (SH) and Nusselt Number (Nu) of the droplets, as estimated by the Ranz-Marshall method, with evaporative equilibrium calculated through Raoult's Law.

9
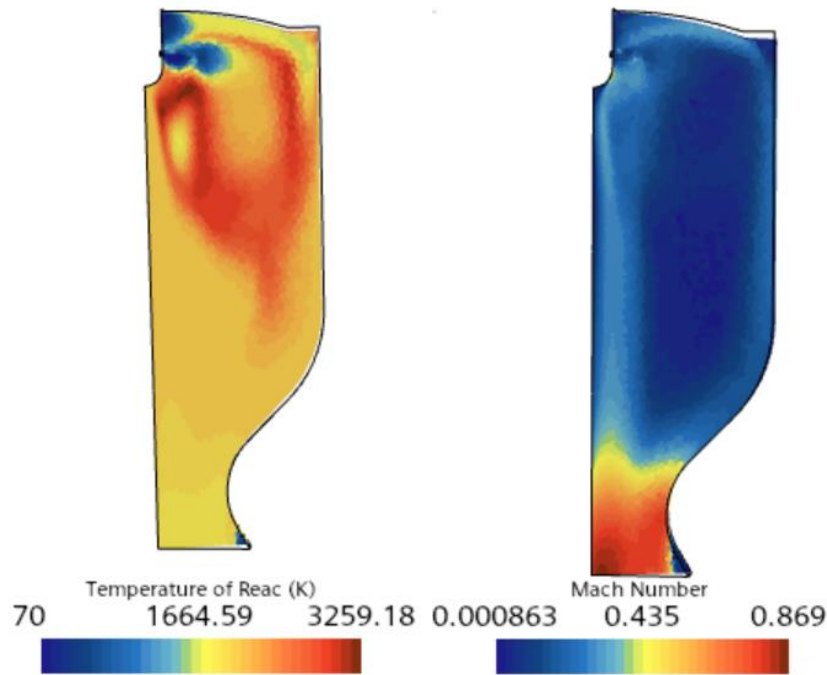
Figure 10: Engine Chamber Gas Temperature and Mach Solutions after 100 Iterations

Current results as shown in Figure 10 demonstrate the ability of this simulation to model evaporative and combustion effects within the flow, as demonstrated by the existence of combustion effects just downstream of the impingement point. However, problems with the simulation persist. As shown in Figure 10, compressible flow within the nozzle has not quite reached convergence for current models, with lower than predicted Mach values at the throat and exit. Irrecoverable divergences occur within the flow simulation by iteration 300, before the compressible flow solution is fully resolved, with point of divergence highly dependent on solver under-relaxation factors. This is likely due to the use of the Segregated Flow solver, which is required for the Eulerian Multiphase model; according to Star documentation, this solver is less robust when it comes to solving compressible flows [4]. Thus, more work will need to be done on tuning the solver metrics and under-relaxation factors to promote compressible convergence with the segregated-type solver.

VIII. Conclusion

After testing, it has been determined that greater stability and lower runtimes for the engine simulation may be achieved through the usage of a reduced chemical mechanism and an Eulerian multiphase flow model. Current efforts are dedicated to increasing stability of the combined steady-state simulation and development of an integrated modeling method for the fluid film evaporation. After these issues are resolved, a transient simulation may be developed using these methods to fully characterize a test firing of the CHROME engine, fulfilling the goal of a high-fidelity digital twin.

IX. Acknowledgments

X. References

[1] Herrera, Manual Jesus, "THE DESIGN AND TESTING OF A 500 LBF LIQUID OXYGEN/LIQUID METHANE ENGINE," Master's Thesis, Department of Mechanical Engineering, University of Texas in El Paso, El Paso, TX, 2019.

[2] David G. Goodwin, Harry K. Moffat, Ingmar Schoegl, Raymond L. Speth, and Bryan W. Weber. "Cantera: An object-oriented software toolkit for chemical kinetics, thermodynamics, and transport processes." https://www.cantera.org, 2022. Version 2.6.0. doi:10.5281/zenodo.6387882

[3] Sutton, G. P., and Biblarz, O., Rocket Propulsion Elements, John Wiley & Sons, Inc, 2016.

[4] Star CCM+ User's Manual. http://www.cd-adapco.com/products/star-ccm/documentation

[5] Frenklach, M. & Wang, Hai & Goldenberg, M. & Smith, Gregory & Golden, D. & Bowman, C. & Hanson, R. & Gardiner, W. & Lissianski, Vitali. (2000). GRI-Mech—An Optimized Detailed Chemical Reaction Mechanism for Methane Combustion.

[6] T.F. Lu & C.K. Law, "A criterion based on computational singular perturbation for the identification of quasi steady state species: A reduced mechanism for methane oxidation with NO chemistry," *Combustion and Flame,* Volume 154, Issue 4, September 2008, Pages 761-774.

[7] B. Franzelli, E. Riber, L.Y.M. Giquel and T. Poinsot, "Large-Eddy Simulation of combustion instabilities in a lean partially premixed swirled flame," *Elsevier,* 5 August 2011.

[8] Prydz, R.; Goodwin, R.D., "Experimental Melting and Vapor Pressures of Methane," *J. Chem. Thermodyn.*, 1972, 4, 1, 127-133, https://doi.org/10.1016/S0021-9614(72)80016-8 .

[9] Brower, G.T.; Thodos, G., "Vapor Pressures of Liquid Oxygen Between the Triple Point and Critical Point", *J. Chem. Eng. Data*, 1968, 13, 2, 262-264, https://doi.org/10.1021/je60037a038